High Resolution Detector Modules Based on NaI(Tl) Arrays for Small Animal Imaging

A.G. Weisenberger, S. Majewski, V. Popov, and R. Wojcik

***Abstract*— We are developing high spatial resolution detector modules based on recently available NaI(Tl) crystal scintillator arrays that are capable of detecting photons over a range of energies. We report on the testing of an array with individual elemet sizes of 1 mm x 1mm arrays over the energy range of 28 keV to 511 keV. It is anticipated that these detector modules could be applied to small animal imaging utilizing single photon emitters such as iodine-125 (28-35 keV) and technetium-99m (140 keV); and also positron emitters such as fluorine-18. The performance of a 5cm square array of NaI(Tl) crystal scintillators in which each element is 1mm x 1mm x 5mm in dimension was measured. The NaI(Tl) array manufactured by Saint-Gobain was coupled to Hamamatsu position sensitive photomultiplier tubes and tested over a range of photon energies. In particular, we tested the NaI(Tl) array with the Hamamatsu model R2487 position sensitive photomultilier tube and the new Hamamatsu model 8500 flat panel position sensitive photomultiplier tube. Though the NaI(Tl) module performed best for the single photon emitters its use in positron emission tomography applications for small animal imaging could be possible even though resulting sensitivity is not ideal.**

I. Introduction

THE crystal scintillator NaI(Tl) has for a long time been used in nuclear medicine applications. The scintillator's high light output makes it ideal for use with the Hamamatsu position sensitive photomultiplier tubes in which the intrinsic position resolution is dependent upon the number of photoelectrons detected. Others and our group have been building detector modules based on arrays of pixelated crystal scintillators such as CsI(Na), CsI(Tl), GSO and LSO coupled to position sensitive photomultiplier tubes for nuclear medicine and animal research applications [1, 2, 3, 4, 5]. The construction of pixelated arrays of NaI(Tl) has been hampered by the hygroscopic nature of the crystal. This new scintillator technology was very recently made available to us from Saint-Gobain Crystals and Detectors (formerly Bicron) [6]. The ability for a single detector module capable of imaging iodine-125, technitium-99m and flourine-18 allows for the construction of a powerful research tool for animal imaging. The radioisotope iodine-125 (I-125) is commonly used in molecular biology and medical research. It is readily available linked to nucleic acids, antibodies and other ligands from companies such as DuPont NEN which provide probes for molecular biology research [7]. The commonly used nuclear medicine isotope technetium-99m (Tc-99m) is readily available and often used in medical research utilizing animals to study disease states. We will report on the results of testing of arrays NaI(Tl) scintillators with I-125, Tc-99m and sodium-22 (Na-22). Tests were made using high resolution copper collimators and a tungsten pinhole collimator.

The Southeastern Universities Research Association (SURA) operates the Thomas Jefferson National Accelerator Facility for the United States Department of Energy under contract DE-AC05-84ER40150.

A.G. Weisenberger, Thomas Jefferson National Accelerator Facility (Jefferson Lab), Newport News, VA (telephone: 757-269-7090, e-mail: drew@jlab.org).

S. Majewski, Jefferson Lab (telephone: 757-269-7448, e-mail: majewski@jlab.org).

V. Popov, Jefferson Lab (telephone: 757-269-6360, e-mail: vpopov@jlab.org).

R. Wojcik, Jefferson Lab (telephone: 757-269-7458, e-mail: wojcik@jlab.org).

II. Measurement Setup

Two different position sensitive photomultiplier tubes were used to measure the performance of a NaI(Tl) scintillating crystal array. One of the PSPMT is the 3" square Hamamatsu R2487 PSPMT which unfortunately is no longer available from Hamamatsu and the other is a prototype of the 4" square Hamamatsu 8500 which is not yet available commercially from Hamamatsu.

A. NaI(Tl) Array

The PSPMTs were optically coupled to the high quality pixelated NaI(Tl) array manufactured by Saint-Gobain Crystals & Detectors. The array is made from optically separated pixels-crystals encapsulated in a compact housing with a 2 mm thick glass window. Table I lists the properties of the array tested. Each NaI(Tl) pixel element is separated by 0.2 mm thick septa made of diffusing white epoxy. An intrinsic energy resolution of 8.97% FWHM @122 keV was measured at the factory using a standard bialkali PMT.

TABLE I
NaI(Tl) Array

Pixel Size	1mm x 1mm x 5mm
Pixel Step	1.25
Number of Pixels	2068 (47 x 44)
Active Size	58.5mm x 54.75mm
External Size	76.3mm x 76.3mm
Window Thickness	75mm
Energy Resolution *	8.97%

*/ Intrinsic energy resolution @122 keV measured at the factory with a standard 2" bialkali PMT and a collimated Co^{57} source.

B. *R2487 PSPMT Based Setup*

The R2487 is a crossed wire anode PSPMT which has 18X and 17Y anodes and an active area of 76 mm x 76 mm. The 12 stage parallel mesh dynode structure results in a gain amplification factor of $1x10^5$. We have reduced the number of channels to readout by connecting neighbor wire anodes into eight anode sectors of six groups of two and two groups of three for the X-anodes. For the Y-anode wires we have seven groups of two neighbor anode wires connected and one group of three connected together. The end result is that we have 8X and 8Y anode sectors to readout.

Studies done with the R2487 were accomplished using the same data acquisition system and image generation methods as we have described elsewhere [1]. Briefly, we make use of LeCroy CAMAC FERA 4300B ADCs to digitize the crosswire anodes of the R2487. The CAMAC system is interfaced via a Jorway SCSI CAMAC crate controller to a Machintosh G3 workstation. On the Macintosh we used the Kmax data acquisition development package from Sparrow Corportation[8].

C. *H8500 PSPMT Based Setup*

We have been evaluating a hybrid variant of the 2" square flat panel H8500 PSPMT which has 64 anodes of the direct output type. We will be publishing the complete results of our evaluation at a future date. The H8500 PSPMT is a 12 stage metal dynode PSPMT with a gain factor of over 10^6 based on a technology similar to the one used in the current generation of compact metal dynode Hamamatsu R5900/R7600/R8520 PSPMTs with active photocathode sizes of 22mm x 22mm. The sample H8500 had a factory-installed high voltage divider and signal connectors for the de-coupled 12th dynode output and for the 64 (8x8) 6 mm x 6 mm anode pads. A 0.1 mm thick μ-metal shield was used around the PSPMT to minimize effect of magnetic fields. Additional in-house built printed circuit boards with readout/amplifier circuitry were attached to the PSPMT through the connectors installed at the back of the factory package. The function of these readout boards is to amplify and invert the dynode signal that is later used to produce a trigger to the ADC data acquisition system; and to de-couple the 64 channel anode pad readout into an 8 X-channel by 8 Y-channel sectorized readout.

The data acquisition system was built around a PC computer using the WindowsNT operating system with a single DATEL PCI 416L ADC card. This PCI computer card is a sixteen channel, 12 bit simultaneous sample-and-hold ADC card with 5 volts input amplitude range [9]. The KmaxNT development software package from Sparrow Corporation was used to develop software to control the acquisition. This control software generates an image by processing the raw anode data on an event by event basis.

D. *Data Acquisition System*

To perform the studies with the two PSPMTs control software developed with the Sparrow Corporation's data acquisition development packages for Macintosh (Kmax) and PC (KmaxNT) based computers was used to generate an images by processing the raw PSPMT data for each scintillation event. Determination of the position of gamma-ray interaction in the scintillator array is determined by computing a truncated center of gravity of the signal distribution on the X and Y anodes of the PSPMT array. This is achieved by using only the digitized signals of those anode wires in the calculation that have a predefined chosen minimal fraction of the sum of all the anode signals (typically 5 to 10%). We have found that the use of this truncated, center-of-gravity (COG) technique is essential to maximizing use of the PSPMT array. The generation of the final processed image is discussed below in the results of I-125 imaging.

III. Test Results

The performance of the 5 cm square array of NaI(Tl) crystal scintillators in which each element is 1 mm x 1 mm x 5 mm in dimension was measured for use with detection of the gamma and x-ray emissions of Na-22, I-125 and Tc-99m. The NaI(Tl) array was coupled to the Hamamatsu R2487 and H8500 position sensitive photomultiplier tubes.

A. *Results from Na-22 studies*

The array of 1 mm x 1 mm x 5 mm NaI(Tl) pixels was optically coupled to a 3" square Hamamatsu R2487 PSPMT. Below in Fig. 1 is shown a flood image obtained by illuminating the face of the detector with 511 keV gamma-rays from a Na-22 source. Also shown are energy spectra obtained with Na-22 (511 and 1274 keV) and Co-57 (122 and 136 keV) source from a single 1 mm x 1 mm x 5 mm scintillation pixel from the central PSPMT region.

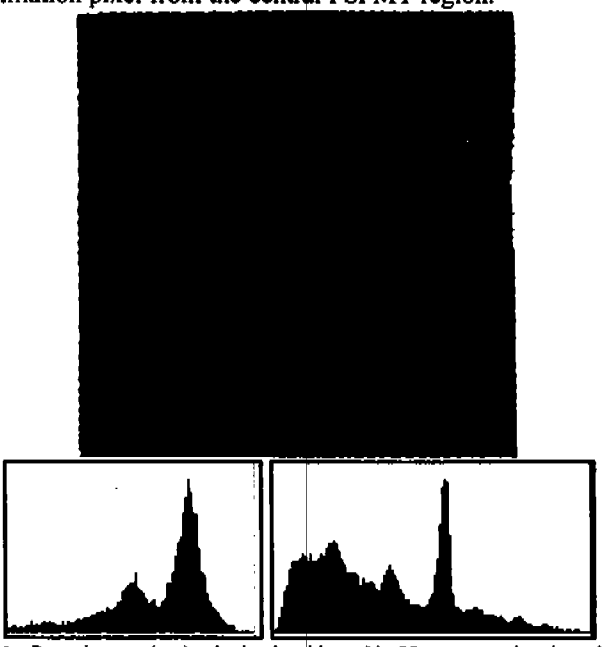

Fig. 1: Raw image (top) obtained with a Na-22 source showing the separation of 1mm x 1mm x 5mm NaI(Tl) pixels. Energy spectra obtained with Co-57 (bottom-left) and Na-22 (bottom-right) source with a single 1mm x 1mm x 5mm scintillation pixel from the central PSPMT region.

The scintillator array was also tested with the H8500 PSPMT. Please see Fig. 2.

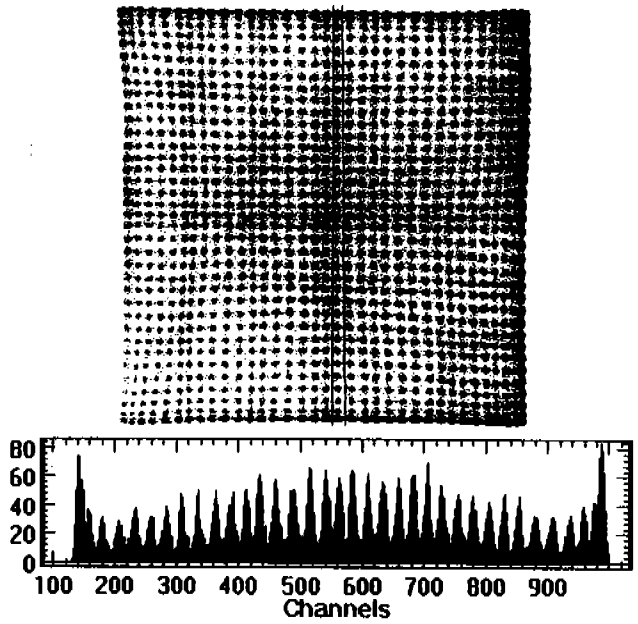

Fig. 2 Top: Raw image obtained with a Na^{22} source. All 34x34 scintillator pixels are well separated. Bottom: Y-projection of the marked vertical pixel column.

The best performance with the H8500 was obtained by directly coupling the array to the PSPMT window. This coupling includes the 2 mm thick window of the array, in addition to the 2.8 mm PSPMT window. Since the active area of the PSPMT is 45mm x 45mm only the center 34 x 34 scintillator elements are in the field of view. In Fig. 2 is shown a raw image obtained with a Na^{22} source that flooded the entire array. All 34 x 34 scintillator pixels are well separated. Also in Fig. 2 is a Y-projection of the marked vertical pixel column. Each individual scintillator pixel element is easily resolved.

B. Imaging of Iodine-125

Because the radioisotope I-125 is commonly used for molecular biology research and is commercially available linked to nucleic acids, antibodies, and other ligands we were particularly interested in the performance of the Na(Tl) array with the detection and imaging of I-125.

To arrive at a final processed image that would be used in a small animal imaging system the results of the X and Y COG calculations to arrive at a raw image are used to identify which crystal of the array detected an event via a crystal map look-up table. The sum of all X and Y anode signals is used to determine if the scintillation event was in the chosen energy window. Each crystal of the array has a defined separate energy acceptance window which is stored in an additional look-up table. The final processed image is formed by incrementing each pixel corresponding to the crystal element.

As can be seen in Figs. 1 and 2, images obtained with PSPMTs exhibit distorted crystal positions because of the spatially non-uniform response of the PSPMT. Since the relative position of each crystal is known and the crystal locations can be defined in the raw image, a distortion correction is achieved by mapping the data identified to belong to a particular crystal into that crystal's appropriate pixel in a corrected image. From the flood image a look-up table was constructed such that individual crystals are identified by mapping their location from the flood image.

The data acquisition system treats the output of each crystal region individually to correct for crystal-to-crystal scintillation output variations as well as local PSPMT gain variations. For each event the sum of the anode signals is used to generate a pulse height energy spectrum. Using an I-125 source an energy calibration is done for each crystal element. Others and ourselves have reported using this method with arrays of scintillating crystals [10, 11]. Finally a flood image is obtained to perform a final flood correction of the mapped image by using an I-125 flood source.

We tested the array coupled to the R2487 PSPMT system with a 0.5mm pinhole tungsten collimator and two parallel hole collimators constructed out of copper and. The low energy radiation of I-125 allows us to use materials other than lead to construct collimators. We have designed a high resolution and a medium resolution parallel hole copper-beryllium collimator. The collimators are constructed out of stacks of layers of copper-beryllium (~1.9% Be) laminates glued together for a total thickness of 0.5 cm. The high resolution copper collimator is 0.5 cm thick and has square openings 0.2 x 0.2 mm^2 in area separated by 0.05 mm thick septa. The medium resolution collimator has square opening 0.75 x 0.75 mm^2 in area separated by 0.16mm thick septa with a total thickness of 0.5 cm. The company, Thermo Electron (Tecomet), constructed the collimator [12].

A simple test phantom was constructed with a total of four glass capillary tubes (see Fig.3).

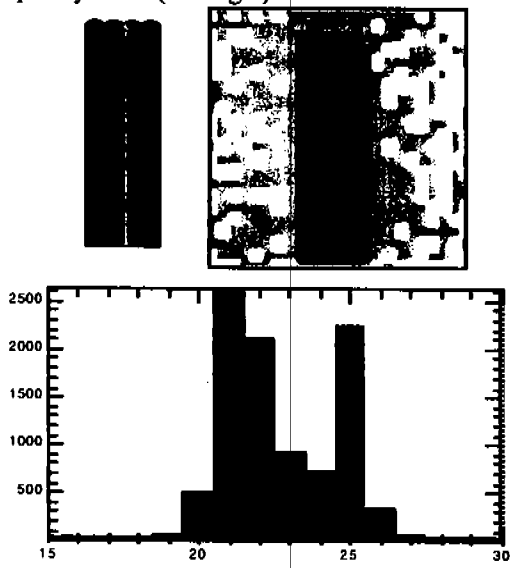

Fig: 3: The simple test phantom (top-left) made with three capillaries filled with I-125 and one empty capillary used as a spacer; center-to-center spacing 1.473mm, i.d.-0.840mm (the dead glass wall separating the two left capillaries was therefore ~0.63mm thick). The high resolution etched copper collimator produced the top-right image. The histogram at the bottom shows a projection along the x-axis of the capillary phantom image.

Three capillaries were filled with I-125 and one empty capillary was used as a spacer. The center-to-center spacing was 1.473 mm, the inner diameter is 0.840 mm. The dead glass wall separating the two left capillaries is therefore ~0.63

mm thick. The phantom was placed in contact with the collimators for all the tests performed with this phantom.

The imaging result using the high resolution etched copper collimator is shown in Fig. 3. The histogram at the bottom shows a projection along the x-axis of the capillary phantom image. In Fig.4 are shown images obtained with the same phantom using the medium resolution etched copper collimator.

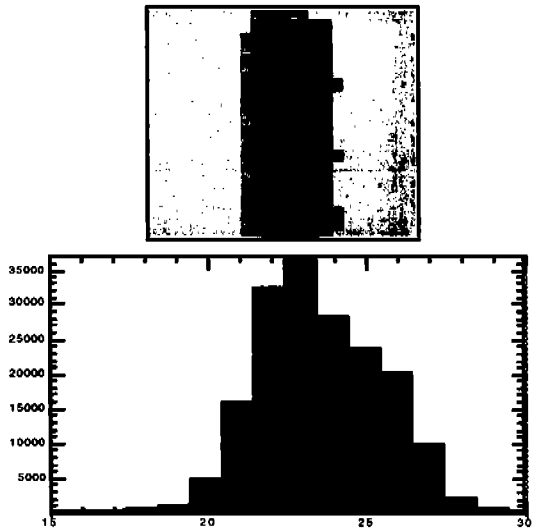

Fig. 4: Medium resolution etched copper collimator produced the above image and an accompanying plot of a projection along the x-axis of the same capillary phantom (note the interference effects of the collimator structure seen in the vertical coordinate).

The 0.5 mm pinhole tungsten collimator was then used to image the capillary phantom. In Fig. 5 shown is the image of the three capillaries produced using a 0.5 mm pinhole with magnification 5. A measured spatial resolution of less than 0.75 mm FWHM was attained in this test. Also displayed is the normalized energy spectrum.

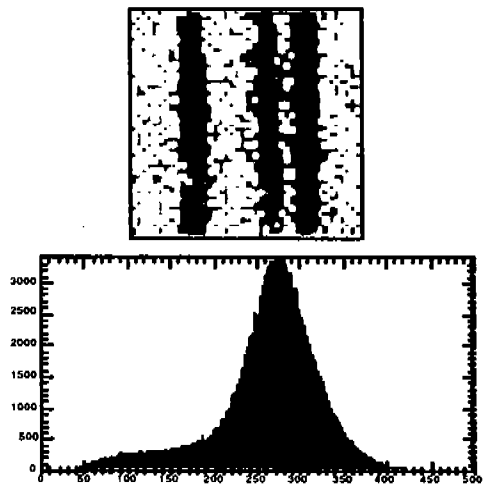

Fig. 5: Shown is an image (top) produced using a 0.5 mm pinhole using a magnification of 5. Note a reversed order of the capillaries in comparison to the previous images. Spatial resolution of less than 0.75 mm FWHM was measured. At the bottom is a normalized energy spectrum.

C. Imaging of Technetium-99m

Finally we tested the array in the application of Tc-99m imaging. The commonly used nuclear medicine isotope is readily used in medical research utilizing animals to study disease states. The energy and flood calibration procedure was done using a Tc-99m source. Images were obtained with the standard high resolution parallel hole lead collimator and the pinhole collimator of the same phantom described above but this time filled with Tc-99m

Results obtained with the high resolution parallel hole lead collimator are shown in Fig.6. The 3.5 cm thick lead collimator has hexagonal opening 1.22 mm in size, with 0.15 mm septa. With this collimator not surprisingly the separation of the capillaries is not fully achieved.

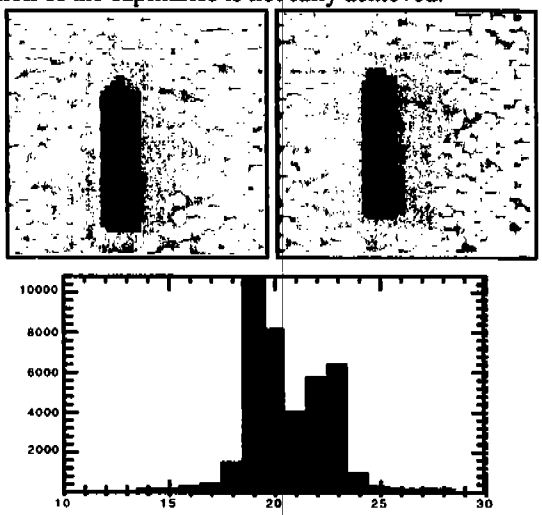

Fig.6: High resolution lead collimator produced images at left for two positions of the capillary phantom and x-projection of the right image (note the reversed order of the capillaries in the image compared to the pinhole collimators).

Resolution measurement results with the pinhole collimator (shown in Fig. 7) resulted in a measured FWHM of the capillaries of 0.75 mm for perpendicular rays to the detector surface.

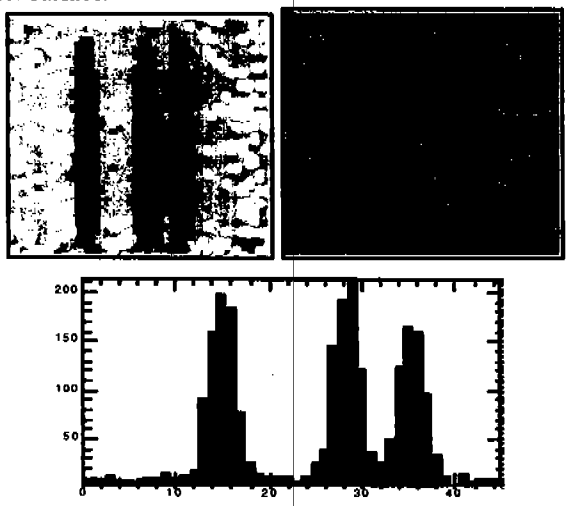

Fig.7: Images produced using a 0.5 mm pinhole collimator. The left image is a raw unprocessed image and the middle image has been filtered and smoothed. The x-projection histogram (right) of the three capillaries obtained with magnification ~5. Resolution eas measured to be 0.75 mm FWHM.

This resolution is only slightly degraded to 0.82 mm FWHM for an impingement angle as large as 35 degrees away from the normal to the detector. This indicates that the depth of interaction effect would not play an important role for 5 mm thick arrays up to at least 140 keV. In the case of thicker (15 mm) arrays more optimal for the PET mode operation, a handle on the depth of interaction effect and the resultant spatial resolution is offered by limiting the reconstruction of the images to the events with a given maximum angle of coincidence.

V. Conclusion

To summarize, we have been developing high spatial resolution detector modules based on recently available NaI(Tl) crystal scintillator arrays from Saint Gobain. We have shown that the array is capable of detecting photons the energy range of 28 keV to 511 keV. It is anticipated that detector modules constructed out of arrays of NaI(Tl) could be applied to small animal imaging utilizing single photon emitters such as iodine-125 (28-35 keV), technetium-99m (140 keV) and positron emitters such as fluorine-18. Though the 5 mm thick NaI(Tl) module performed best for the single photon emitters its ability to be used in positron emission tomography applications for small animal imaging could be possible even though resulting sensitivity is not ideal.

IV. Acknowlegment

We thank Hamamatsu Photonics for providing us with the sample of the flat panel H8500 PSPMT.

Daniel Herr and Tim Parker from Saint Gobain Crystals and Detectors are thanked for providing us with prototypes of their high quality scintillator arrays used in this study.

V. References

[1] R. Wojcik, S. Majewski, D. Steinbach and A.G. Weisenberger, "High Spatial Resolution Gamma Imaging Detector Based on 5'' Diameter R3292 Hamamatsu PSPMT," *IEEE Transactions on Nuclear Science*, vol. 45, no. 3, pp. 487-491, June, 1998.

[2] R.Pani, F.Scopinaro, G.Depola, R.Pellegrini, A.Soluri; "Very High Resolution Gamma Camera Based on Position Sensitive Photomultiplier Tube," *Physica Medica*, vol 9. no. 2-3, pp. 233-236, 1993.

[3] A. Truman, A.J. Bird, D. Ramsden and Z. He, "Pixellated CsI(Tl) arrays with position-sensitive PMT readout," *Nucl. Instr. and Meth A*, 353(1994) pp. 375-378, 1994.

[4] A.G. Weisenberger, B. Kross, S. Majewski, R. Wojcik, E. Bradley, and M. Saha, "Design Features and Performance of a CsI(Na) Array Based Gamma Camera for Small Animal Gene Research," *IEEE Trans. on Nuclr. Sci*, vol. 45, no. 6, pp. 3053-3058, December 1998.

[5] M.B. Williams, V. Galbis-Reig, A.R. Goode, P.U. Simoni, S. Majewski, A. G. Weisenberger, R. Wojcik, W. Phillips, M. Stanton, "Multimodality Imaging of Small Animals," *RSNA Electronic Journal*, 1999 (http://ej.rsna.org/ej3/0107-99.fin/dual99.htm).

[6] Saint-Gobain Crystals and Detectors, (Bicron), Hillsborough, NJ.

[7] NEN® Research Products Catalog, DuPont NEN, June 1994.

[8] Sparrow Corporation, Daytona Beach, Fl, www.sparrowcorp.com

[9] Datel Inc, Mansfield, MA, www.datel.com

[10] D. Steinbach, S. Majewski, M. Williams, B. Kross, A.G. Weisenberger and R. Wojcik, "Development of a Small Field of View Scintimammography Camera Based on a YAP Crystal Array and a Position Sensitive PMT", *Conf. Rec of the 1996 IEEE NSS/MIC*, pp. 1251-1256, 1997.

[11] J.L. Robar, C.J. Thompson, K. Murthy, R.L. Clancy and A.M. Bergman, "Correction of Spatial Distortion, Gain Nonuniformity and Efficiency Variation in Detectors for Positron Emission Mammography," *Conf. Rec of the 1996 IEEE NSS/MIC*, pp. 1206-1210, 1997.

[12] Thermo Electron -Tecomet, Precision Assemblies Operations, Woburn, MA.